

Supplementary Material: Deregulated FASN Expression in BRAF Inhibitor-Resistant Melanoma Cells Unveils New Targets for Drug Combinations

Serena Stamatakos, Giovanni Luca Beretta, Elisabetta Vergani, Matteo Dugo, Cristina Corno, Elisabetta Corno, Stella Tinelli, Simona Frigerio, Emilio Ciusani, Monica Rodolfo, Paola Perego and Laura Gatti

Text S1: Cell Migration and Invasion Assay

The assays were carried out as previously described, with minor modifications [1]. Cells were seeded (8×10^5 per well) to 24-well transwell chambers (Costar, Corning Inc., Corning, NY, USA) in serum-free medium; in the bottom well the complete medium was added. For invasion assays, the transwell membranes were previously coated with 12.5 μ g matrigel per well (BD Biosciences, Franklin Lakes, NJ, USA) and dried for 1 h. After 24 h of incubation at 37 °C, cells that migrated to the lower chamber or invaded the matrigel and then migrated to the lower chamber were fixed in 95% ethanol, stained with a solution of 0.4% sulforhodamine B (SRB, Sigma–Aldrich, St. Louis, MO, USA) in 1% acetic acid, and counted under an inverted microscope.

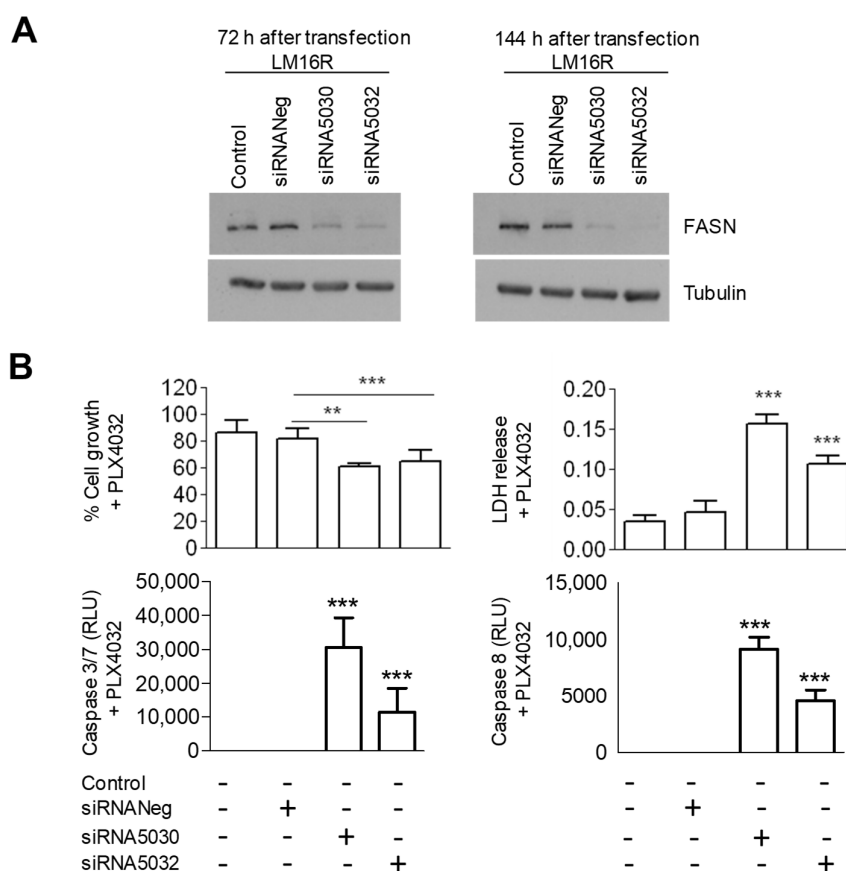


Figure S1. Expression of FASN in relation to resistance to BRAF. inhibitors. (A) Cells were transfected with FASN-directed siRNAs. The levels of FASN were evaluated by western blotting 72 h after transfection, when drug treatment started, and at the end of the experiment (144 h after transfection). Equal loading of SDS-PAGE is shown by tubulin. (B) Seventy two hours after transfection, cells were analyzed in terms of sensitivity to PLX4032 (3 μ M) by CCK8 assay and LDH assay, and by caspase 3/7 and caspase 8 activation assays. ** $P < 0.01$, *** $P < 0.0001$ by one-way ANOVA followed by Bonferroni correction.

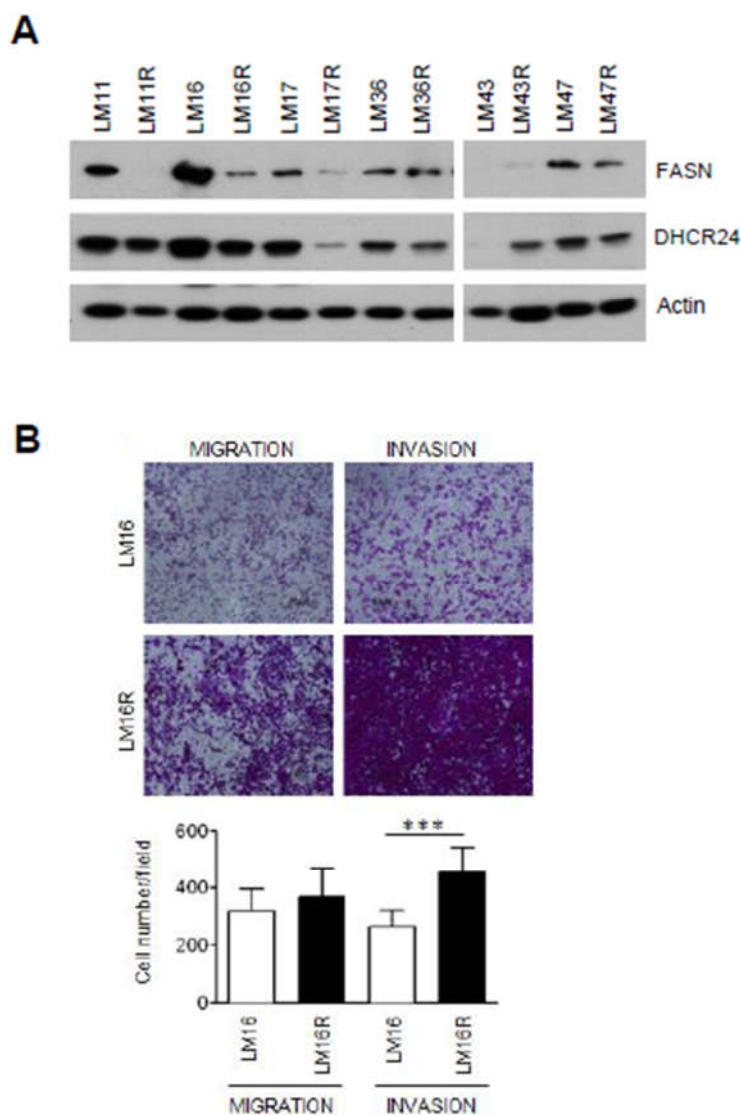


Figure S2. (A) Expression of FASN and DHCR24 in relation to. resistance to BRAF inhibitors. Western blot analysis of FASN and DHCR24 levels in sensitive and resistant cell lines. Equal loading is shown by actin. (B) Representative images of migration and invasion assays in serum-free medium using transwell plates. Migrating and invading cells were counted under a light microscope. Columns represent cell numbers/field (\pm SE; $n = 3$). *** $P < 0.001$ by unpaired Student's t test.

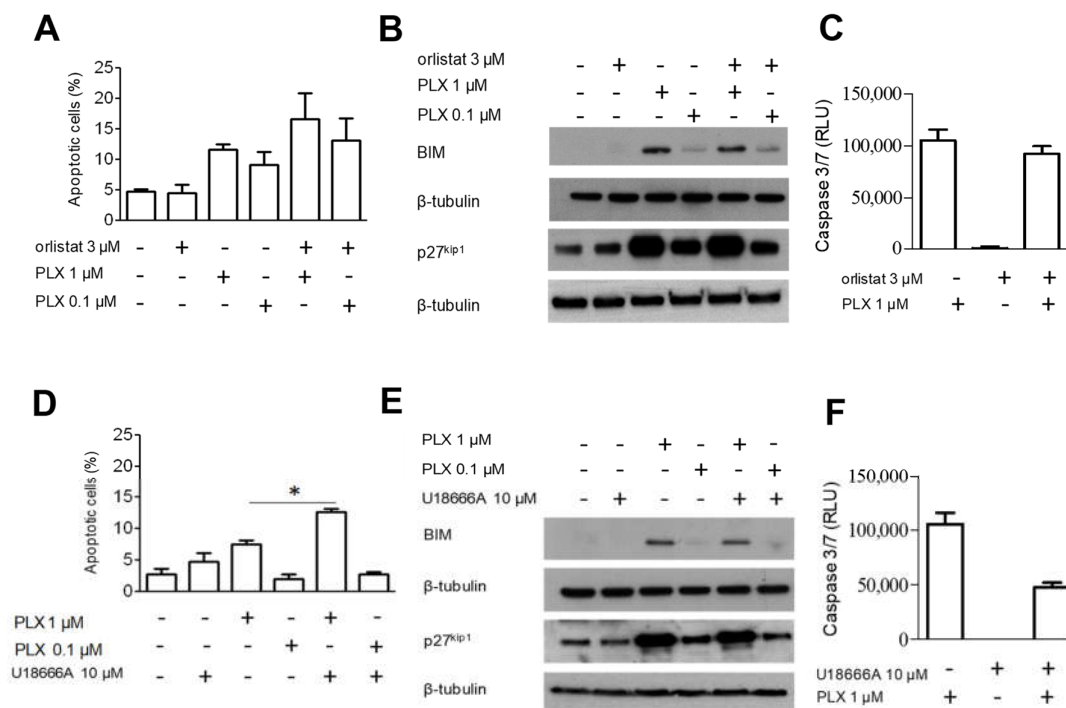


Figure S3. Effect of the combination of PLX4032, orlistat and U18666A in LM16 cells. (A–D), LM16 cells were exposed to single agents or to their combination and harvested 48 h after treatment for analysis of apoptotic response by Annexin V-binding assay. * $P < 0.05$ by one-way ANOVA followed by Bonferroni correction. (B–E), Western blot analyses in LM16 cells exposed to the drugs alone or in combination for 48 h. Equal loading is shown by tubulin. (C–F), Caspase 3/7 activation evaluated in LM16 cells treated with PLX4032 alone or in combination with orlistat or U18666A by subtracting the control levels. * $P < 0.05$ by one-way ANOVA followed by Bonferroni correction compared to single agents.

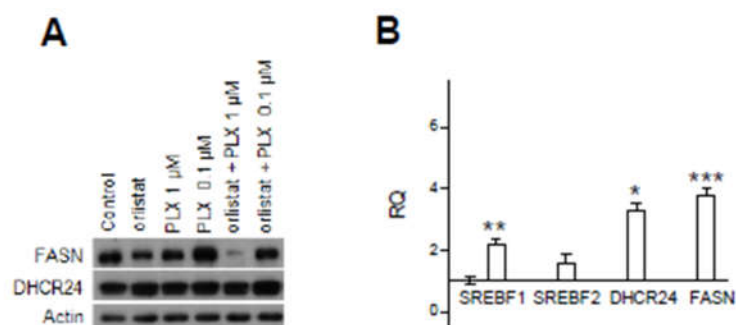


Figure S4. Effects of FASN inhibition on DHCR24 regulation in LM16 cells. (A) FASN and DHCR24 levels after 48 h treatment with orlistat (3 μ M) and PLX4032 as single agents or in combination. Equal loading is shown by actin. (B) Expression levels of SREBF1, SREBF2, DHCR24 and FASN as determined by qRT-PCR in LM16 cells upon treatment with orlistat (3 μ M). Relative quantification (RQ) values are shown. * $P < 0.05$, ** $P < 0.01$, *** $P < 0.0001$ by unpaired Student's t test compared to the vehicle (DMSO)-treated.

Table S1. List of BRAF-mutated melanoma cell lines in CCLE database.

| CCLE_ID | depMapID | Name | Histology | BRAF_mutation | PLX4720 IC50 (μ M) |
|--------------|------------|----------|--------------------|---------------|-------------------------|
| A2058_SKIN | ACH-000788 | A2058 | malignant_melanoma | p.V600E | 8 |
| A375_SKIN | ACH-000219 | A-375 | malignant_melanoma | p.V600E | 0.258287698 |
| C32_SKIN | ACH-000580 | C32 | malignant_melanoma | p.V600E | 2.206977606 |
| COLO679_SKIN | ACH-000805 | COLO-679 | malignant_melanoma | p.V600E | 0.554165304 |

| | | | | | |
|----------------|------------|-------------|--------------------|-------------------------|-------------|
| COLO741_SKIN | ACH-000582 | COLO 741 | malignant_melanoma | p.V600E | 4.03970623 |
| G361_SKIN | ACH-000572 | G-361 | malignant_melanoma | p.V600E | 1.286707997 |
| HS294T_SKIN | ACH-000014 | Hs 294T | malignant_melanoma | p.V600E | 8 |
| HS695T_SKIN | ACH-000799 | Hs 695T | malignant_melanoma | p.V600E | 7.264561176 |
| HS939T_SKIN | ACH-000814 | Hs 939.T | malignant_melanoma | p.V600E | 2.102822304 |
| HT144_SKIN | ACH-000322 | HT-144 | malignant_melanoma | p.V600E | 1.336324811 |
| IGR37_SKIN | ACH-000650 | IGR-37 | malignant_melanoma | p.V600E | 0.904429674 |
| IGR39_SKIN | ACH-000550 | IGR-39 | malignant_melanoma | p.V600E | 8 |
| K029AX_SKIN | ACH-000404 | K029AX | malignant_melanoma | p.V600E | 2.110589266 |
| LOXIMVI_SKIN | ACH-000750 | LOX IMVI | malignant_melanoma | p.V600E;p.I208V | 8 |
| MALME3M_SKIN | ACH-000477 | Malme-3M | malignant_melanoma | p.V600E | 0.285528094 |
| MDAMB435S_SKIN | ACH-000884 | MDA-MB-435S | malignant_melanoma | p.V600E | 2.312842846 |
| MELHO_SKIN | ACH-000450 | MEL-HO | malignant_melanoma | p.V600E | 0.312976211 |
| RPMI7951_SKIN | ACH-000348 | RPMI-7951 | malignant_melanoma | p.V600E | 8 |
| RVH421_SKIN | ACH-000614 | RVH-421 | malignant_melanoma | p.V600E | 0.770638406 |
| SKMEL24_SKIN | ACH-000822 | SK-MEL-24 | malignant_melanoma | p.V600E | 5.15450716 |
| SKMEL31_SKIN | ACH-000640 | SK-MEL-31 | malignant_melanoma | p.V600E | 8 |
| SKMEL5_SKIN | ACH-000730 | SK-MEL-5 | malignant_melanoma | p.V600E | 0.369111031 |
| UACC257_SKIN | ACH-000579 | UACC-257 | malignant_melanoma | p.V600E | 1.064142346 |
| UACC62_SKIN | ACH-000425 | UACC-62 | malignant_melanoma | p.V600E | 0.249700621 |
| WM115_SKIN | ACH-000304 | WM-115 | malignant_melanoma | p.V600V;p.V600E;p.V600D | 8 |
| WM1799_SKIN | ACH-000661 | WM1799 | malignant_melanoma | p.V600E | 1.226397991 |
| WM2664_SKIN | ACH-001239 | WM-266-4 | malignant_melanoma | p.V600V;p.V600E;p.V600D | 1.578695059 |
| WM793_SKIN | ACH-000827 | WM-793 | malignant_melanoma | p.V600E | 8 |
| WM88_SKIN | ACH-000899 | WM-88 | malignant_melanoma | p.V600E | 0.204083994 |
| WM983B_SKIN | ACH-000765 | WM-983B | malignant_melanoma | p.V600E | 0.51123476 |

Table S2. Analysis of the drug interaction between PLX4032 and orlistat or PLX4032 and U18666A in LM16 cells¹.

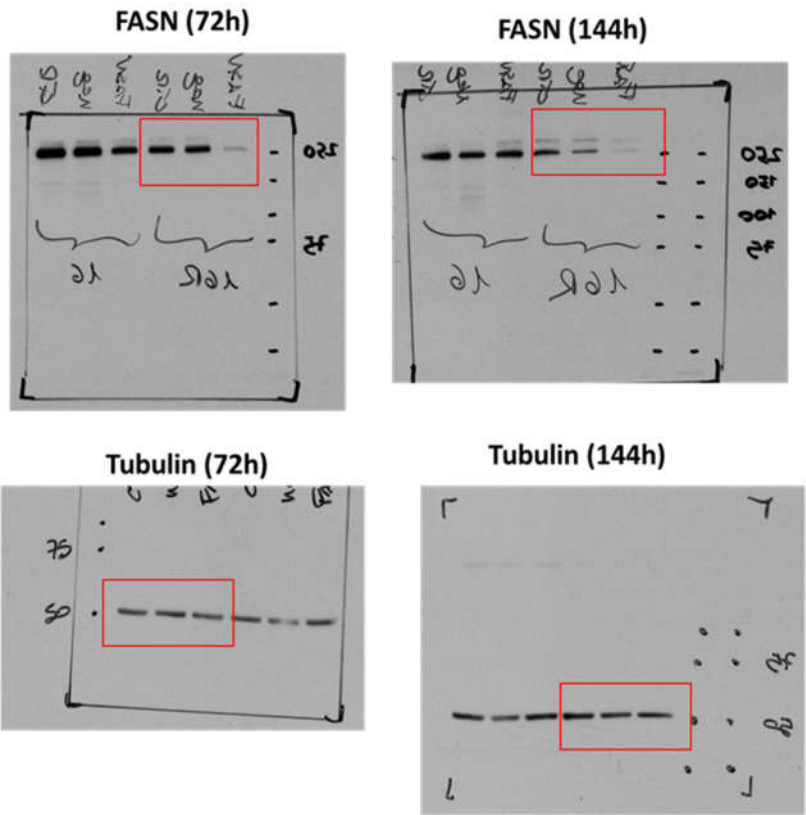
| - | CI ² | | | |
|---------|--------------------|--------------------|--------------------|---------------|
| PLX4032 | 3 μM orlistat | 10 μM orlistat | 3 μM U18666A | 10 μM U18666A |
| 10 μM | 2.97 ± 0.81 | 4.53 ± 3.00 | 2.67 ± 1.23 | 3.40 ± 0.78 |
| 1 μM | 0.6 ± 0.18 | 0.67 ± 0.40 | 0.72 ± 0.10 | 1.17 ± 0.19 |
| 0.1 μM | 0.23 ± 0.18 | 0.94 ± 0.68 | 1.68 ± 1.14 | 2.14 ± 0.68 |
| 0.01 μM | 31.06 ± 12.75 | 3.34 ± 0.52 | 17.35 ± 19.85 | 2.83 ± 0.88 |

¹, Cell sensitivity was assessed by cell growth inhibition assay. Cells were seeded and 24 h later exposed to each drug and to their simultaneous combination for 72 h. Cells were then counted using a cell counter. ², The drug interaction was analyzed by the Chou and Talalay method, calculating a combination index (CI) and CI values indicating synergistic drug interactions are in bold. Mean CI values \pm SE of three independent experiments are reported.

Table S3. Analysis of the drug interaction between PLX4032, orlistat and U18666A in LM16 cells¹.

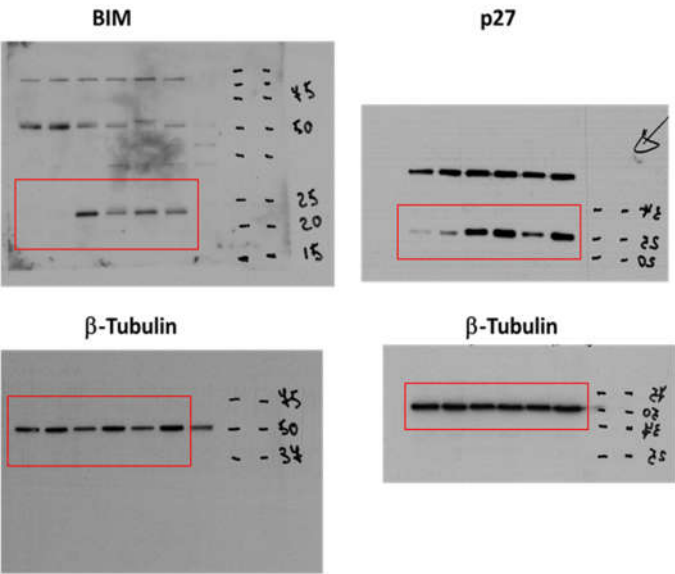
| PLX4032 | orlistat (μ M) | U18666A (μ M) | CI ² |
|--------------|---------------------|--------------------|-----------------------------------|
| 0.1 μ M | 10 μ M | 10 μ M | 1.11 \pm 0.13 |
| 0.1 μ M | 10 μ M | 3 μ M | 0.67 \pm 0.07 |
| 0.1 μ M | 3 μ M | 10 μ M | 1.4 \pm 0.96 |
| 0.1 μ M | 3 μ M | 3 μ M | 0.41 \pm 0.02 |
| 0.01 μ M | 10 μ M | 10 μ M | 0.96 \pm 0.18 |
| 0.01 μ M | 10 μ M | 3 μ M | 1.06 \pm 0.32 |
| 0.01 μ M | 3 μ M | 10 μ M | 0.86 \pm 0.21 |
| 0.01 μ M | 3 μ M | 3 μ M | 4.90 \pm 3.60 |

¹, Cell sensitivity was assessed by cell growth inhibition assay. ², Combination Index (CI) values showing synergistic drug interactions are reported in bold. CI are the mean \pm SE of three independent experiments.



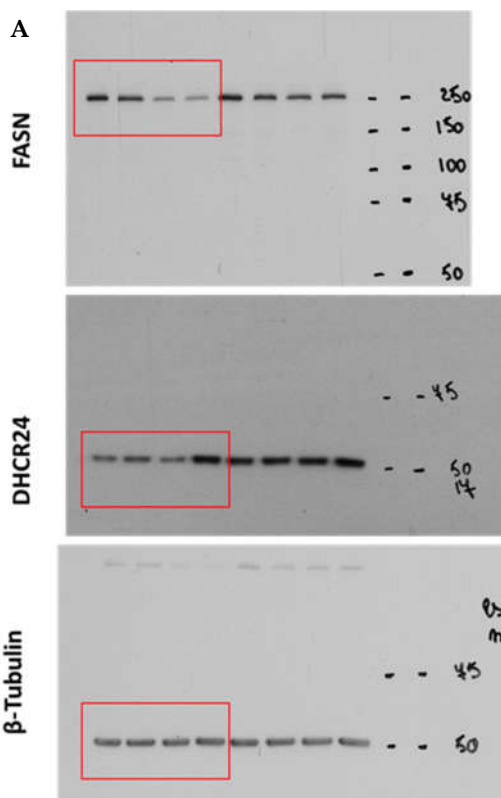
| Name | FASN | Tubulin | FASN/Tub |
|----------------------|-----------|-----------|-------------|
| LM16R CTR 72h | 127426020 | 74338867 | 1.714123784 |
| LM16R siRNA Neg 72h | 124549035 | 71666862 | 1.737888775 |
| LM16R siFASN 72h | 35576396 | 63207505 | 0.56285082 |
| LM16R CTR 144h | 142853257 | 101872687 | 1.402272397 |
| LM16R siRNA Neg 144h | 106147120 | 71882698 | 1.47667134 |
| LM16R siFASN 144h | 10724711 | 71544124 | 0.14990345 |

Figure S5. Densitometric analysis was used to measure the band intensity (Figure 1A). The relative expression levels (ratio between the band intensity of FASN and the corresponding band intensity of tubulin) was determined by ImageQuant 5.2 software.



| Name | BIM | Tubulin | BIM/Tub | p27 | Tubulin | p27/Tub |
|------------------------------------|----------|----------|----------|-----------|-----------|----------|
| Control | 2010433 | 32166158 | 0.062501 | 30510668 | 136545134 | 0.223447 |
| Orlistat 3 μ M | 2072734 | 43911430 | 0.047203 | 49963595 | 127961429 | 0.390458 |
| PLX 1 μ M | 29204735 | 30437774 | 0.95949 | 120242560 | 127325274 | 0.944373 |
| PLX 0,1 μ M | 26407246 | 35806485 | 0.737499 | 140637886 | 134499052 | 1.045642 |
| Orlistat 3 μ M/PLX 1 μ M | 30158109 | 27188883 | 1.109207 | 74996051 | 126729961 | 0.591778 |
| Orlistat 3 μ M/PLX 0,1 μ M | 23825512 | 39033819 | 0.610381 | 127618264 | 146163452 | 0.87312 |

Figure S6. Densitometric analysis was used to measure the band intensity (Figure 2B). The relative expression levels (ratio between the band intensity of BIM or p27 and the corresponding band intensity of tubulin) was determined by ImageQuant 5.2 software.



| Name | FASN | Tubulin | DHCR24 | FASN/Tub | DHCR24/Tub |
|-----------|----------|----------|----------|-------------|-------------|
| Control | 23558677 | 21766672 | 15567568 | 1.082327928 | 0.71520203 |
| siRNANeg | 25182525 | 22490675 | 15473418 | 1.119687382 | 0.687992601 |
| siRNA5030 | 18079820 | 21400241 | 13068710 | 0.844841888 | 0.610680506 |
| siRNA5032 | 20323428 | 29542737 | 29002517 | 0.687933146 | 0.981713949 |

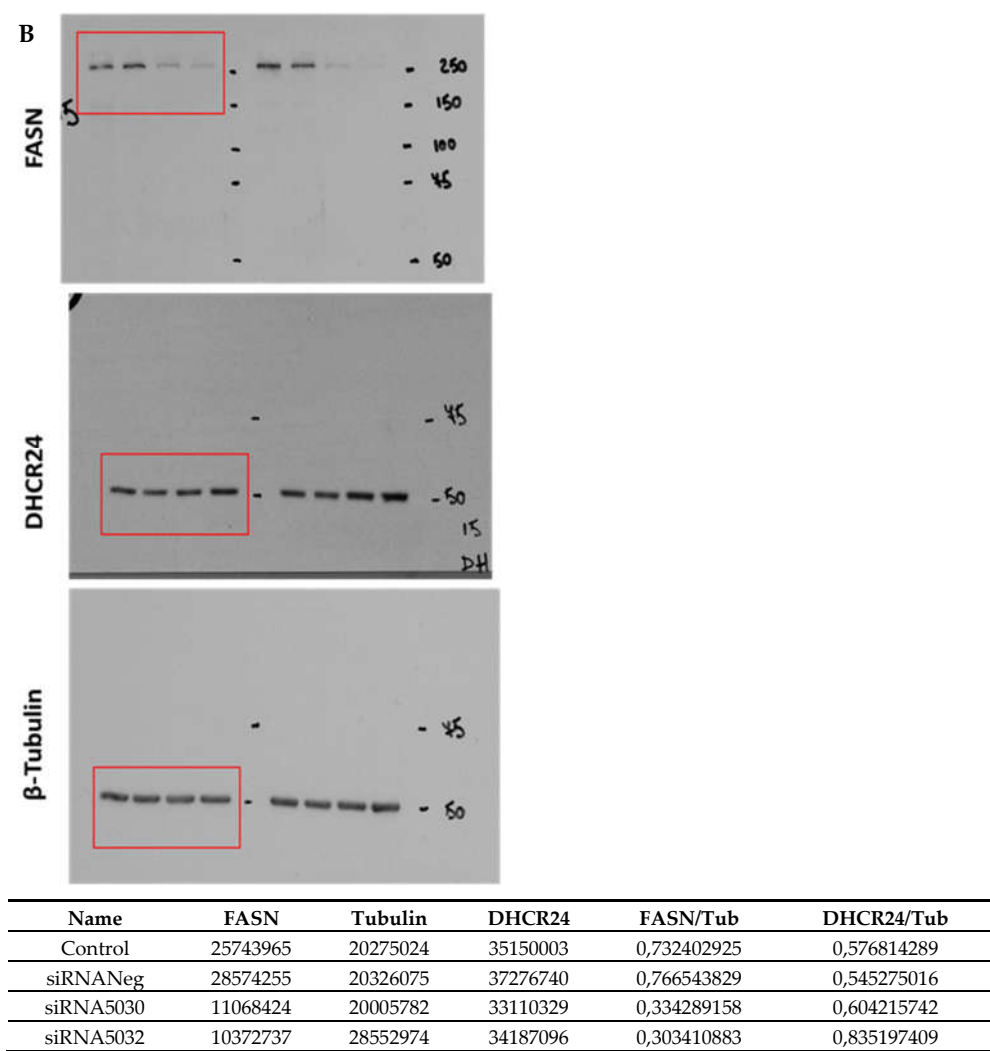
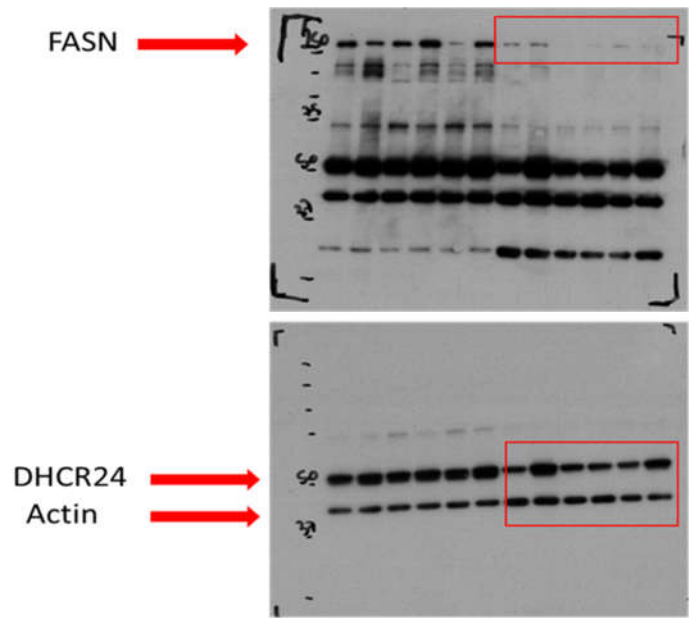


Figure S7. Densitometric analysis was used to measure the band intensity (Figure 3A). (A–B) The relative expression levels (ratio between the band intensity of FASN or DHCR24 and the corresponding band intensity of tubulin) was determined by ImageQuant 5.2 software.



| Name | FASN | Actin | DHCR24 | FASN/Act | DHCR24/Act |
|-----------------------------------|---------|----------|----------|----------|------------|
| Control | 1723548 | 16907673 | 16469137 | 0.101939 | 0.974063 |
| Orlistat 3 μ M | 2438740 | 17332794 | 27145421 | 0.140701 | 1.566131 |
| PLX 30 μ M | 72778 | 16779087 | 17629673 | 0.004337 | 1.050693 |
| PLX 10 μ M | 280213 | 17230945 | 14398530 | 0.016262 | 0.83562 |
| Orlistat 3 μ M/PLX 30 μ M | 753527 | 13037288 | 12562238 | 0.057798 | 0.963562 |
| Orlistat 3 μ M/PLX 10 μ M | 151607 | 11949388 | 21196815 | 0.012687 | 1.773883 |

Figure S8. Densitometric analysis was used to measure the band intensity (Figure 3B). The relative expression levels (ratio between the band intensity of FASN or DHCR24 and the corresponding band intensity of actin) was determined by ImageQuant 5.2 software.

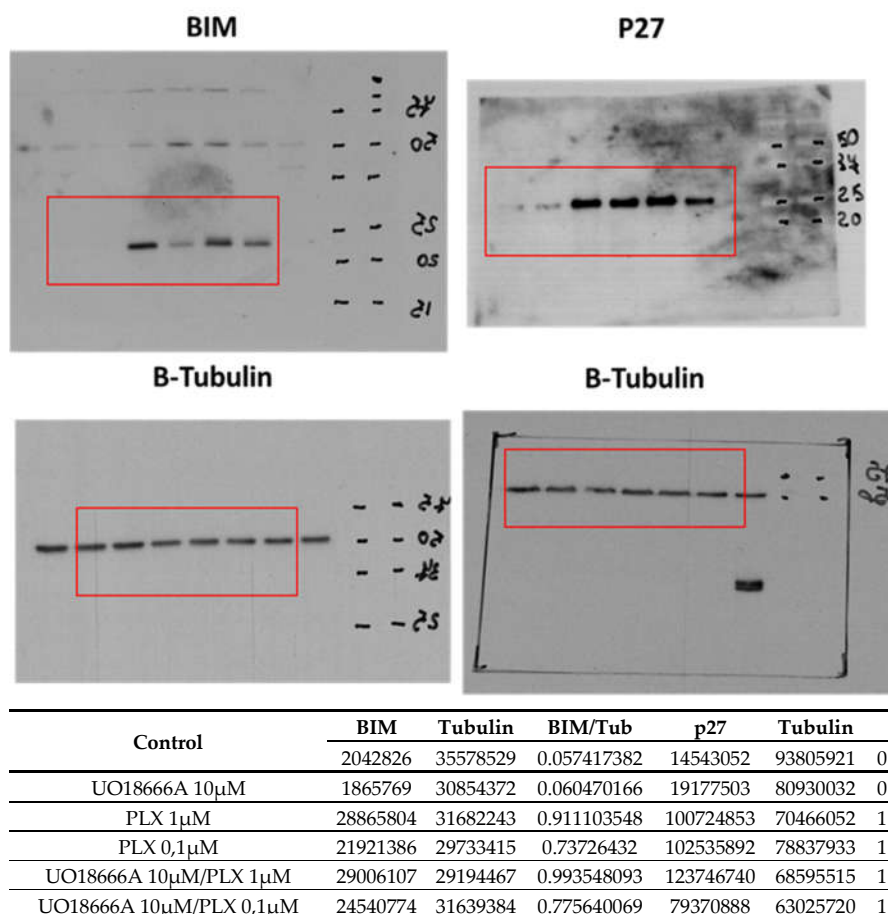


Figure S9. Densitometric analysis was used to measure the band intensity (Figure 4B). The relative expression levels (ratio between the band intensity of BIM or p27 and the corresponding band intensity of tubulin) was determined by ImageQuant 5.2 software.

References

1. Cassinelli, G.; Lanzi, C.; Petrangolini, G.; Tortoreto, M.; Pratesi, G.; Cuccuru, G.; Laccabue, D.; Supino, R.; Belluco, S.; Favini, E.; Poletti, A.; Zunino, F. Inhibition of c-Met and prevention of spontaneous metastatic spreading by the 2-indolinone RPI-1. *Mol Cancer Ther.* **2006**, *5*, 2388–2397, doi:10.1158/1535-7163.MCT-06-0245.

Publisher's Note: MDPI stays neutral with regard to jurisdictional claims in published maps and institutional affiliations.



© 2021 by the authors. Licensee MDPI, Basel, Switzerland. This article is an open access article distributed under the terms and conditions of the Creative Commons Attribution (CC BY) license (<http://creativecommons.org/licenses/by/4.0/>).